Institute for
Naval Oceanography

TM-5
OCTOBER 1991

THE UTILITY OF ACOUSTIC TRAVEL TIMES IN LOCATING THE NORTH WALL OF THE GULF STREAM

MICHAEL S. FOSTER, CDR, USN

Institute for
Naval Oceanography

THE UTILITY OF ACOUSTIC TRAVEL TIMES IN LOCATING THE NORTH WALL OF THE GULF STREAM

MICHAEL S. FOSTER, CDR, USN

TABLE OF CONTENTS

Abstract

Eighty-seven days of travel time data for ocean acoustic transmissions across the north wall of the Gulf Stream were examined. The data was collected from 7 July to 1 October 1990 during the 1990 Applied Tomography Experiment (ATE90), sponsored by the Chief of Naval Research. The acoustic ray paths were, generally, perpendicular to the north wall. The analysis indicates that acoustic ray travel times can be useful in locating ocean frontal features and in reliably augmenting subjective techniques based on infrared (IR) satellite imagery and bathythermograph (BT) data. This document presents the procedures employed during the study and discusses the results.

THE UTILITY OF ACOUSTIC TRAVEL TIMES IN LOCATING THE NORTH WALL OF THE GULF STREAM

Introduction

The principal objective of the Applied Tomography Experiment 1990 (ATE 90) was to apply tomographic techniques to long distance ocean acoustic transmission data with the goal of improving performance predictions for Navy antisubmarine warfare (ASW) systems. That objective is being pursued by several investigators under the sponsorship of the Chief of Naval Research with the Applied Physics Laboratory, University of Washington (APL/UW) as the principal performer. The structural plan for ATE90 presented the opportunity to 1) examine the effect of fronts and eddies on measured acoustic ray travel time and 2) investigate the relationship between acoustic travel time variations and the spatial movement of these strong gradient ocean features. This study examines the potential for acoustic ray travel time measurements to make a direct, real time contribution to the Navy's oceanographic requirements.

During the period 7 July through 1 October, 1990, acoustic ray travel time data were collected in the North Atlantic Ocean in support of ATE90. The Institute for Naval Oceanography (INO), in the 19 April 1990 (revised 24 May 1990) task plan which defined Naval Oceanographic and Atmospheric Research Laboratory (NOARL) and Naval Oceanographic Office (NAVOCEANO) support for ATE90, was charged to assess the utility of acoustic tomographic data in determining the location of the Gulf Stream front (north wall) using a synoptic oceanography approach employing frequent tomographic (acoustic travel time) observations. Part of the task was to compare the INO results with the location of the Gulf Stream as determined by the Operational Oceanography Center (OOC) of NAVOCEANO without using tomographic data, and to evaluate the differences with meaningful statistics and measures of performance. The methods and procedures employed in this study were straightforward and, therefore, should be easily understood by those with minimal exposure to the fields of oceanography and acoustics. The results point to a simple, easily applied technique for tracking not only fronts such as the north wall of the Gulf Stream, but also, other strong temperature gradient features (e.g., eddies) throughout the world's oceans.

Experiment Description

Acoustic transmissions at 250 hertz were initiated from a deeply moored source near Bermuda. Several Navy-owned arrays, located more than 1000 kilometers away were used as the receivers. After preliminary processing, the signal data was forwarded to APL/UW where it was further processed into the format used in this study. Of the source-receiver combinations incorporated in the plan for ATE90, only one (labelled P1006) provided reliable data consisting of 6 ray paths. The NAVOCEANO OOC provided IR satellite imagery and subjective sea surface temperature (SST) analysis charts of the Gulf Stream region traversed by line P1006. This study is confined to data collected for line P1006.

A constant value has been subtracted from all absolute travel time data presented in this report. This paper will focus on a study of travel time changes (deltas) and those parameters which may be derived. Fortunately, acoustic travel time deltas are adequate to test the hypothesis that, under certain conditions, the position of the north wall of the Gulf Stream can be located and tracked by employing acoustic measurement techniques.

The acoustic source transmitted a signal at four hour intervals except for two one-week periods during which the transmissions were repeated at 40 minute intervals. Daily 0000 Universal Standard Time travel times were extracted to form two data subsets for analysis, one consisting of 24-hour acoustic travel time values for the first arriving (fastest) ray, and the second composed of averaged travel time values for all six rays. Using these subsets, 24-hour time difference (ΔT) values were calculated. Each ΔT value was then converted to a distance parameter (ΔR) using the empirical relationship

$$\Delta R = - \Delta T * (1 \text{ km} / .005 \text{ seconds}).$$

Spiesberger (1989) determined that each 5-millisecond change in acoustic travel time closely approximates a spatial variation of 1 kilometer. Since values of ΔR, alone, do not effectively demonstrate the meandering nature of north wall movement, running ΔR summations were calculated which would hopefully demonstrate high correlation with the meandering behavior of the north wall. Since operational constraints did not permit anchoring of running summations of ΔR values to physical reference points, the data set averages (sample means) for the derived cumulative data were subtracted to create a common reference point of zero. The above steps were accomplished for the average travel times of all six P1006 rays and for the first arriving ray.

The SST analyses prepared by the NAVOCEANO OOC, that were input to the Optimum Thermal Interpolation System (OTIS), were used to tabulate a third data set consisting of along-slice spatial ΔR values for north wall movement. The cumulative sample mean for these ΔR values was subtracted to conform with the zero-based reference frame of the acoustically derived values. IR satellite imagery (when cloud free) was also reviewed to verify the OOC SST analyses. Finally, the ΔR values derived from acoustic travel time and their running summation were compared with the tabulated deltas and summations derived from the OOC SST analyses.

Data Analysis

The complete acoustic data set will not be published here, in deference to the principle investigators of ATE90; however, the Appendix presents the acoustic travel times for source/receiver path P1006 and the derivations therefrom, which form the basis for this study. Likewise, signal characteristics and array geometry will not be discussed in this document.

Figures 1 through 4 illustrate the variation in north wall position as calculated from acoustic travel time measurements and as derived from OOC subjective analyses. Figures 1 and 2 are based on the averaged travel time for all six acoustic ray arrivals along source-receiver path P1006. Figures 3 and 4 are similar to Figures 1 and 2; however, the plots represent only the first arriving (fastest) ray. Figures 1 and 3 are similar in that both are non-cumulative plots of daily delta values for the 6-ray average and first arriving ray, respectively. Figures 2 and 4 depict the respective cumulative representation of the plots in Figures 1 and 3.

It is readily apparent that the spatial deltas derived from the OOC analyses oscillate with greater amplitude and higher frequency than their acoustically derived counterparts. The acoustically measured deltas (6-ray average) and the OOC deltas were like signed, i.e., positive vs. negative, on only 27 out of 87 days, far less than might be expected. The cumulative plots depicted in Figures 2 and 4 contain the accumulation of errors contributed by individual data points. Over time, these errors are additive, producing a subtle deviation of each plot from reality. In addition, a consistent error is introduced at the outset by initializing each plot to its mean value on Julian Day 189 (7 July 1990). This artificiality does, however, effectively minimize the separation between the two plotted data points for each day.

In a positive sense, it is encouraging to find that the absolute value for all daily ΔR values derived from acoustic travel times were less than 55.56 km/day (30 nautical miles/day). Seventy-eight of the 86 NAVOCEANO OOC subjectively derived ΔR values were within this range. The mean absolute values of ΔR for the first arriving rays, the 6-ray averages and the OOC subjective analyses were 7.5, 7.1, and 14.9 km/day, respectively. If the subjective analyses are taken as ground truth (a somewhat risky assumption), it would seem appropriate to change the previously discussed empirical formulation to reflect a 2.5 (vice 5) millisecond correspondence to a 1 kilometer spatial variation, in order to bring the acoustically derived values into closer agreement with the subjective analyses. However, this would not be a realistic endeavor since there is no other experimental evidence to support such a modification. The OOC analyses are primarily a reflection of the top few meters of the ocean, while the acoustically derived ΔR values incorporate both vertical and horizontal sampling of the ocean, in an integral sense.

Perhaps the most impressive characteristic of the acoustically derived values for ΔR is the smoothness of their behavior. Their cumulative plots (Figures 2 and 4) indicate only 4 major minima and 4 maxima over the entire 86 day period. The cumulative record from the OOC analyses is more sawtooth in its behavior, making it difficult to develop a criteria for use in classifying the maxima and minima. Sign changes within the ΔR records are also a revealing indication of smoothness. Table I illustrates a smoothness parameter (n), which is based on the number of sign changes (s) among the N data points of the three data sets used in this study. As s ranges between zero (no sign changes) and N-1 (maximum number of sign changes), n varies with values between 1 and 0. Table I indicates the acoustic data to be more than 10% smoother than the subjective data using this criterion.

Table I. Smoothness of ΔR data sets based upon the number of sign changes (s) contained in each data set (N cases).

DATA SOURCE	NO. SIGN CHANGES (s)	SMOOTHNESS PARAMETER (n) $= [(N-s-1)/N-1]$
ΔR(6-RAYS)	11	0.87
ΔR(1ST RAY)	15	0.82
ΔR(OOC)	23	0.73

Table II presents the results of statistical analysis as applied to the data sets, both singularly and jointly. Of particular interest are the cross correlations between acoustically derived ΔR values and the OOC deltas. There is a definite indication that the OOC analysis lags the real time acoustic measurement by 2 days. This lag is attributable, in part, to the fact that the OOC performs its full-fledged analysis three times per week. The availability and application of acoustic travel time measurements on a real time basis should be useful in eliminating this apparent phase shift between the OOC analysis and the continuously changing position of the north wall.

Results

The differences between the acoustically derived and OOC analysis positions are, in large part, attributable to cloud cover, which often prevents satellite observation of the sea surface. In the absence of cloud free satellite data, analysts must rely almost exclusively upon persistence and experience to define SST contours. The relative north wall positions derived from acoustic travel times, on the other hand, reflect the application of a simple arithmetical formula to produce a record of change which is free of the subjectivity inherent in manual analysis techniques. The behavior of the two data sets (acoustic derivation and subjective analysis) clearly demonstrates that, accuracy notwithstanding, use of acoustic travel times to locate the north wall offers improved consistency. The error growth inherent in continuous summation of ΔR values can be avoided through periodic adjustments and/or use of actual frontal positions.

Table II. Data set statistical measurements.

a. Delta values (sample mean not subtracted).

	N	MIN	MAX	MEAN	STD. ERR.	STD. DEV.
AVERAGE(6-RAYS)	86	-25.880	17.700	-1.136	0.958	8.833
FIRST ARRIVING RAY	86	-45.680	19.900	-1.363	1.066	9.828
OOC ANALYSIS	86	-88.896	55.560	0.258	2.563	23.632

b. Cumulative delta values (sample mean subtracted).

	N	MIN	MAX	MEAN	STD. ERR.	STD.DEV.
AVERAGE (6-RAYS)	86	-56.184	97.177	0	4.256	39.239
FIRST ARRIVING RAY	86	-54.763	101.217	0	4.636	42.745
OOC ANALYSIS	86	-129.595	103.755	0	5.063	46.680

c. Cross Correlations (sample mean not subtracted).

LAG	AVERAGE (6-RAYS) vs. OOC ANALYSIS	FIRST ARRIVING RAY vs. OOC ANALYSIS
NONE	17.271	25.992
1 DAY	29.171	27.695
2 DAYS	35.770	40.708
3 DAYS	23.819	8.881
4 DAYS	21.338	13.879

Caution must be exercised in arriving at further conclusions regarding the value of travel time data as a means of locating strong gradient ocean features such as the north wall of the Gulf Stream. Subjectivity in the OOC analyses tends to mask actual movement of the north wall while the complexity of the ocean temperature structure lends its own measure of discordance to the acoustically derived ΔR values. Rudimentary efforts to assess the vertical and horizontal complexity of the ray path led to inconclusive results, in both cases, as described in the following discussions.

Vertical Ray Path Considerations:

Classically, the earliest arriving ray has the greatest vertical amplitude and, therefore, experiences greater variability in watermass structure during its journey from source to receiver. This ray spends more time near the surface where the horizontal temperature gradient through the north wall is strongest. In addition, this ray probes to greater depths where the ocean temperature structure is relatively homogeneous and more nearly constant with respect to time. Therefore, one may reason that the travel time of this ray should more accurately reflect changes in the north wall position. Support for this line of reasoning was not evident in the ATE90 data set, as may be seen by comparing the cumulative delta plots given in Figures 2 and 4. Here, the plots are seemingly identical and it is only by comparing the individual daily deltas plotted in Figures 1 and 3 that the small differences between the 6-ray average and the first arriving ray become apparent. It seems reasonable to expect that ray tracing and tomographic techniques, when applied to the complete ray path travel time data, can resolve these small differences and produce useful positioning information.

Horizontal Ray Path Considerations:

As an integral measurement, the travel time of a given ray represents a sampling of the entire watermass along the path between source and receiver. If the ray should pass through a cold core eddy south of the north wall, the acoustic travel time would be expected to increase (lower sound speed), thereby simulating a more southerly position of the north wall. The opposite is true when a warm core eddy north of the front is traversed by a ray. In this case, a more northerly position for the north wall would be indicated by the acoustic travel time.

Given the existence of two homogeneous watermasses separated by a sharp boundary, changes in the travel time of acoustic energy across the boundary are the result of dynamic processes at the boundary. In a simplistic sense, the north wall of the Gulf Stream may be regarded as such a boundary and its spatial movement as the main reason for variation in acoustic travel time. However, the boundary of the north wall is only infrequently such a simple feature. Warm and cold core eddies/rings must be considered in the boundary definition.

It seems useful to categorize the complexity of the north wall boundary to assist in analyzing the acoustic travel time along a given cross section or slice. A simple classification system consists of four cases as shown in Figure 5: (1) no eddies, (2) a warm core eddy, (3) a cold core eddy, and (4) both warm and cold core eddies. In the case where no eddies occur along the ray path, application of the empirical algorithm to monitor north wall movement requires no modification beyond periodic realignment with satellite imagery. To achieve success in the other cases requires (at a minimum) knowledge of the spatial extent of the eddies bisected by the ray path. If the ray path passes through an eddy, the absolute change in acoustic travel time is proportional to the extent of the ray path lying within the eddy. This distance should be subtracted from the ΔR value derived from the empirical calculation if the eddy is warm core and added if the eddy is cold core. The presence of multiple fronts and complex undulations in the north wall introduces considerations not covered by the above classification system.

An attempt was made to modify acoustically derived ΔR values using the classification scheme discussed above and depicted in Figure 5; however, using the OOC analyses for this purpose introduced the same subjectivity into the revised ΔR data sets as exists in the original ΔR data derived from the OOC analyses. The results were inconclusive and suggest the need for additional algorithms similar to the one used in this study.

Conclusion

Acoustic travel time measurements are of immediate benefit in tracking strong gradient features between relatively homogeneous watermasses when no eddy interference is present. This information is especially useful for tracking the north wall of the Gulf Stream during cloudy or even partly cloudy periods when the view of the ocean surface in satellite IR imagery is obstructed. Further investigation is needed to identify techniques for applying travel time measurements in cases involving complex frontal structures. While it may be some time before tomographic techniques are incorporated into ocean models and acoustic travel time measurements can be assimilated into them, the measurements offer, potentially, a direct and immediate return on investments in ocean acoustic transceiver systems. As a direct measurement of the behavior of acoustic energy, sound travel time is capable of improving and augmenting the operational analysis of boundary features such as the north wall of the Gulf Stream.

References

Spiesberger, J.L. (1989). Remote Sensing of Western Boundary Currents Using Acoustic Tomography. J. Acoust. Soc. Am. 86(1), 346-351.

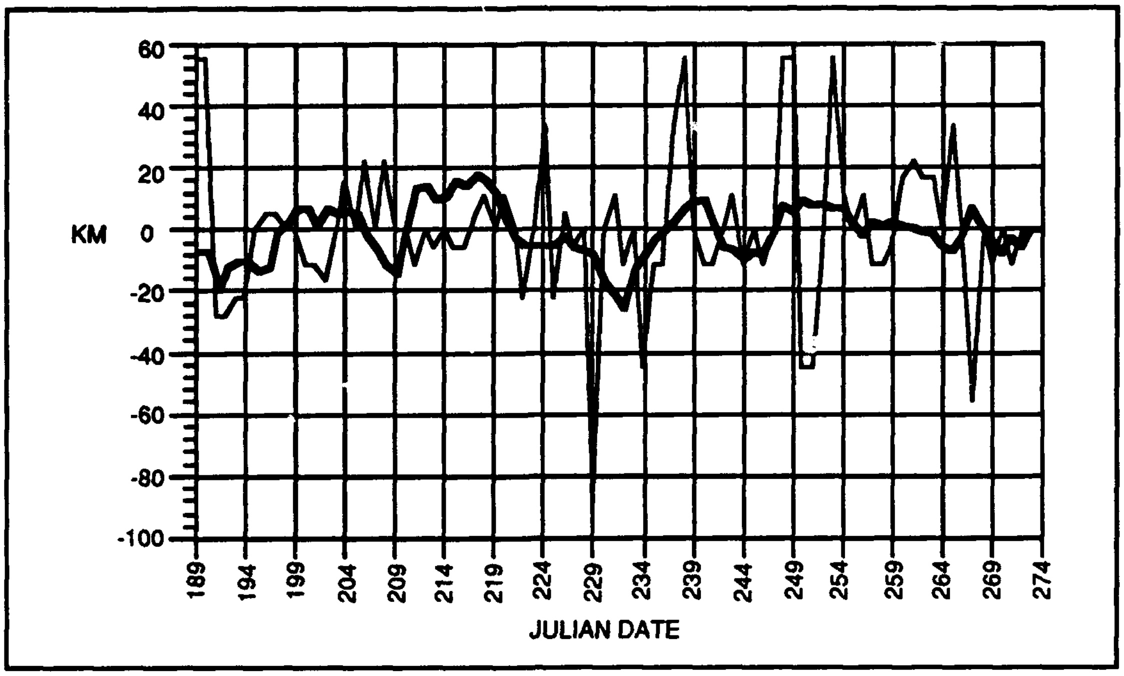

Figure 1. Daily variation in ΔR as calculated from the 6-ray average of acoustic travel times for ray path P1006 (bold plot) vs. daily spatial movement of the north wall of the Gulf Stream per the OOC subjective analysis (fine plot). Julian dates 189 and 274 correspond to 8 July and 1 October 1990, respectively.

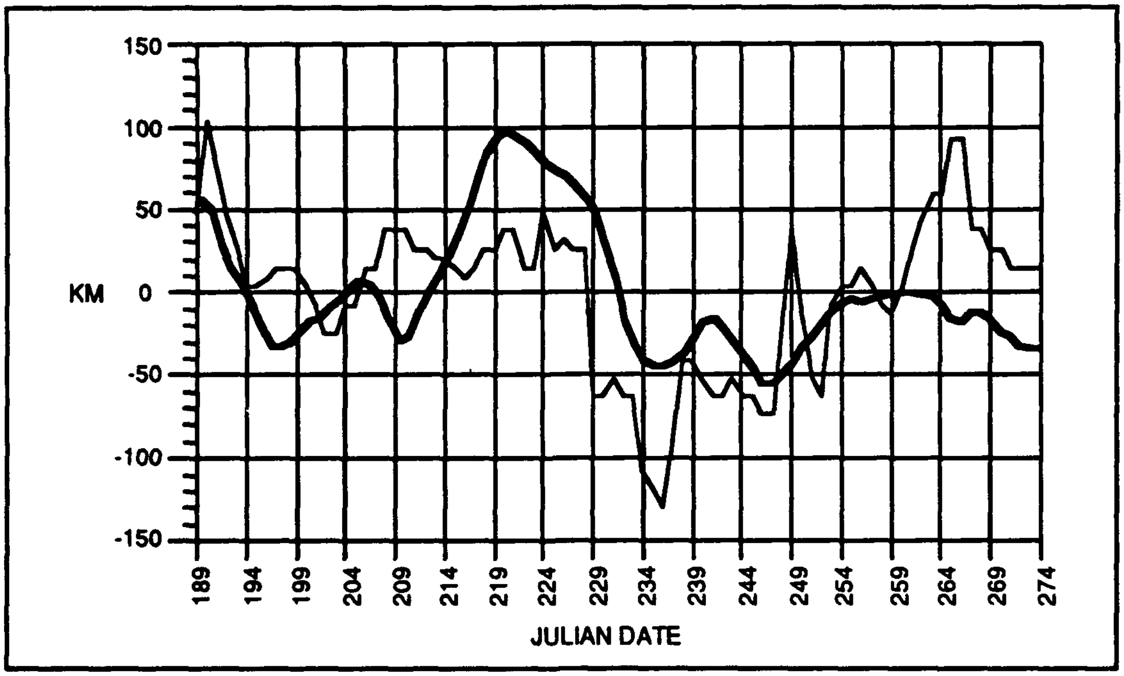

Figure 2. Cumulative plot of daily variations in ΔR as calculated from the 6-ray average of acoustic travel times for ray path P1006 (bold plot) vs. cumulative daily spatial movement of the north wall of the Gulf Stream per the OOC subjective analysis (fine plot). Julian dates 189 and 274 correspond to 8 July and 1 October 1990, respectively.

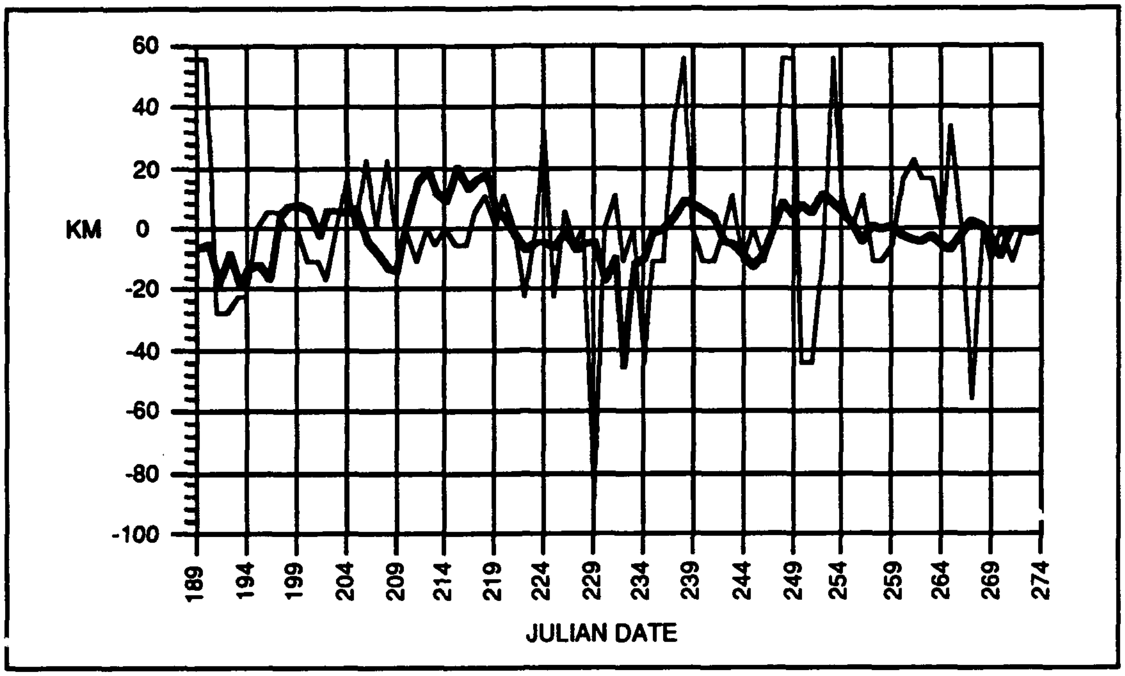

Figure 3. Daily variation in ΔR as calculated from the acoustic travel time of the first arriving ray for ray path P1006 (bold plot) vs. daily spatial movement of the north wall of the Gulf Stream per the OOC subjective analysis (fine plot). Julian dates 189 and 274 correspond to 8 July and 1 October 1990, respectively.

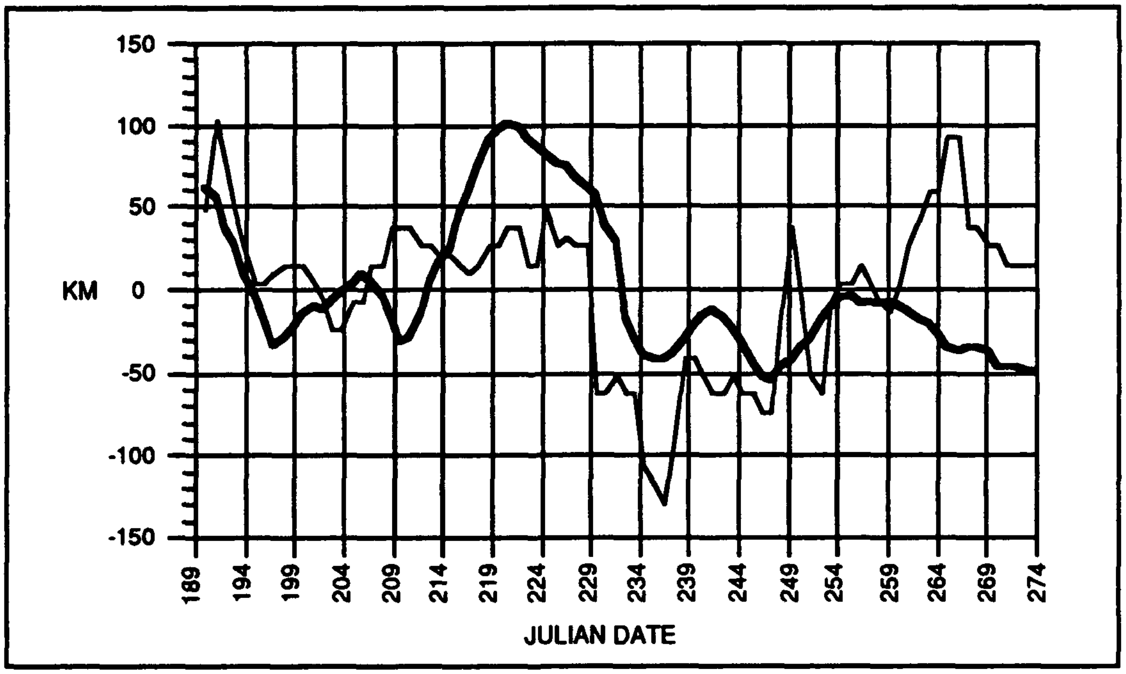

Figure 4. Cumulative plot of daily variation in ΔR as calculated from the acoustic travel time of the first arriving ray for ray path P1006 (bold plot) vs. cumulative daily spatial movement of the north wall of the Gulf Stream per the OOC subjective analysis (fine plot). Both time series have been modified by subtracting the data set means from each data point. Julian dates 189 and 274 correspond to 8 July and 1 October 1990, respectively.

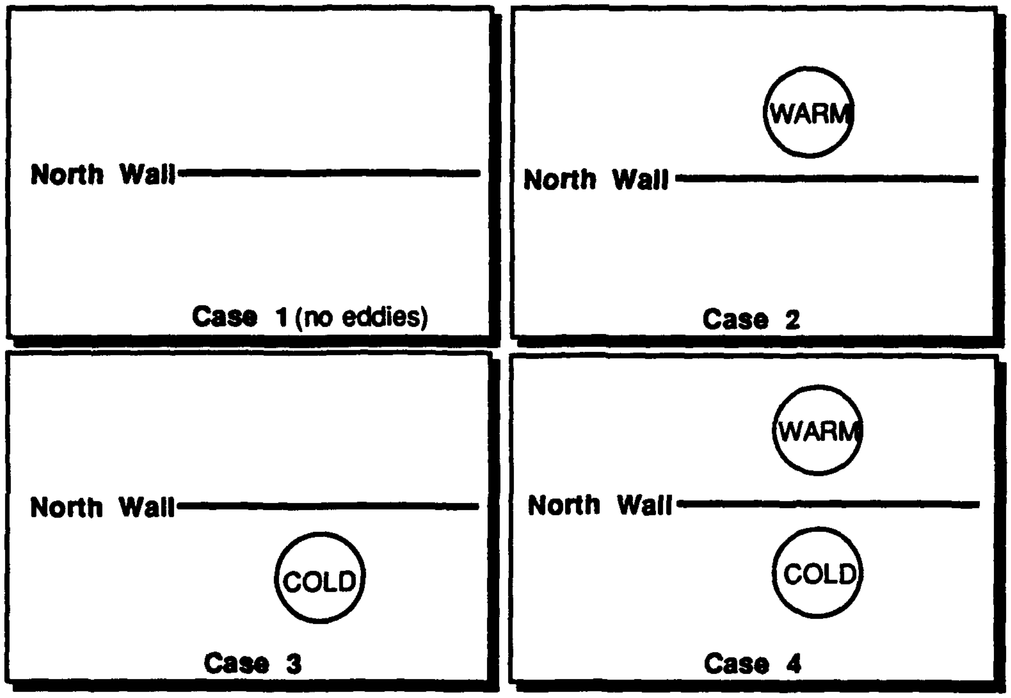

Figure 5. Classification of the frontal features of the north wall of the Gulf Stream.

Appendix

Relevant Data Sets

Section I. Data collected and calculated for the first arriving acoustic ray. Columns per the following description:

Column A: JULIAN DATE - 189 and 274 correspond to July 7 and 1 October 1990, respectively.

Column B: ACOUSTIC TRAVEL TIME measurement in seconds (Note: a constant value has been subtracted).

Column C: 24-HOUR ACOUSTIC ΔT in seconds (current value minus value from previous day).

Column D: 24-HOUR ΔR in kilometers, calculated from the value in column C.

Column E: CUMULATIVE ΔR in kilometers (summation of current and all previous values in column D).

Column F: CUMULATIVE ΔR in kilometers (value in column E minus the average of all values in column E).

A	B	C	D	E	F
189	28.816401	0.032801	-6.560135	-6.560135	60.837105
190	28.843100	0.026699	-5.339813	-11.899948	55.497292
191	28.935900	0.092800	-18.560028	-30.459976	36.937264
192	28.980400	0.044500	-8.900070	-39.360046	28.037194
193	29.074100	0.093700	-18.740082	-58.100128	9.297112
194	29.141500	0.067400	-13.479996	-71.580124	-4.182884
195	29.202499	0.060999	-12.199783	-83.779907	-16.382667
196	29.286600	0.084101	-16.820145	-100.600050	-33.202810
197	29.265900	-0.020700	4.140091	-96.459961	-29.062721
198	29.232500	-0.033400	6.679916	-89.780045	-22.382805
199	29.193800	-0.038700	7.740021	-82.040024	-14.642784
200	29.167200	-0.026600	5.319977	-76.720047	-9.322807
201	29.180000	0.012800	-2.560043	-79.280090	-11.882850
202	29.153700	-0.026300	5.260086	-74.020004	-6.622764
203	29.127501	-0.026199	5.239868	-68.780136	-1.382896
204	29.101700	-0.025801	5.160141	-63.619995	3.777245
205	29.070601	-0.031099	6.219864	-57.400131	9.997109
206	29.093800	0.023199	-4.639816	-62.039947	5.357293
207	29.139099	0.045300	-9.059906	-71.099853	-3.702613
208	29.205400	0.066301	-13.260269	-84.360122	-16.962882
209	29.277399	0.071999	-14.399719	-98.759841	-31.362601
210	29.266800	-0.010599	2.119827	-96.640014	-29.242774
211	29.190500	-0.076300	15.259933	-81.380081	-13.982841

Section I (continued)

A	B	C	D	E	F
212	29.096500	-0.094000	18.799973	-62.580108	4.817132
213	29.037800	-0.058701	11.740112	-50.839996	16.557244
214	28.993601	-0.044199	8.839798	-42.000198	25.397042
215	28.894100	-0.099501	19.900131	-22.100067	45.297173
216	28.829100	-0.065001	13.000107	-9.099960	58.297280
217	28.750299	-0.078800	15.760040	6.660080	74.057320
218	28.662201	-0.088099	17.619705	24.279785	91.677025
219	28.633301	-0.028900	5.780029	30.059814	97.457054
220	28.614500	-0.018801	3.760147	33.819961	101.217201
221	28.627899	0.013399	-2.679825	31.140136	98.537376
222	28.664400	0.036501	-7.300186	23.839950	91.237190
223	28.688601	0.024200	-4.840088	18.999862	86.397102
224	28.711399	0.022799	-4.559708	14.440154	81.837394
225	28.743900	0.032501	-6.500244	7.939910	75.337150
226	28.750099	0.006199	-1.239777	6.700133	74.097373
227	28.786400	0.036301	-7.260132	-0.559999	66.837241
228	28.814100	0.027700	-5.540085	-6.100084	61.297156
229	28.838600	0.024500	-4.899979	-11.000063	56.397177
230	28.928400	0.089800	-17.959976	-28.960039	38.437201
231	28.979099	0.050699	-10.139847	-39.099886	28.297354
232	29.207500	0.228401	-45.680237	-84.780123	-17.382883
233	29.267500	0.059999	-11.999893	-96.780016	-29.382776
234	29.318399	0.050900	-10.179901	-106.959920	-39.562680
235	29.328400	0.010000	-2.000046	-108.959960	-41.562720
236	29.330000	0.001600	-0.320053	-109.280020	-41.882780
237	29.313400	-0.016600	3.319931	-105.960090	-38.562850
238	29.268499	-0.044901	8.980179	-96.979906	-29.582666
239	29.229900	-0.038599	7.719803	-89.260103	-21.862863
240	29.201300	-0.028601	5.720139	-83.539964	-16.142724
241	29.183500	-0.017799	3.559875	-79.980089	-12.582849
242	29.206301	0.022800	-4.560089	-84.540178	-17.142938
243	29.233299	0.026999	-5.399704	-89.939882	-22.542642
244	29.276699	0.043400	-8.679962	-98.619844	-31.222604
245	29.342199	0.065500	-13.100052	-111.719900	-44.322660
246	29.385300	0.043100	-8.620071	-120.339970	-52.942730
247	29.394400	0.009100	-1.819992	-122.159960	-54.762720
248	29.352301	-0.042099	8.419800	-113.740160	-46.342920
249	29.330700	-0.021601	4.320145	-109.420010	-42.022770
250	29.292900	-0.037800	7.559967	-101.860050	-34.462810
251	29.268600	-0.024300	4.859924	-97.000123	-29.602883
252	29.212200	-0.056400	11.280060	-85.720063	-18.322823
253	29.172501	-0.039700	7.939911	-77.780152	-10.382912
254	29.145800	-0.026701	5.340195	-72.439957	-5.042717

Section I (continued)

A	B	C	D	E	F
255	29.139900	-0.005899	1.179886	-71.260071	-3.862831
256	29.162300	0.022400	-4.479980	-75.740051	-8.342811
257	29.158001	-0.004299	0.859833	-74.880218	-7.482978
258	29.159901	0.001900	-0.379944	-75.260162	-7.862922
259	29.155199	-0.004702	0.940323	-74.319839	-6.922599
260	29.167101	0.011902	-2.380371	-76.700210	-9.302970
261	29.188200	0.021099	-4.219818	-80.920028	-13.522788
262	29.210100	0.021900	-4.380035	-85.300063	-17.902823
263	29.224501	0.014400	-2.880096	-88.180159	-20.782919
264	29.255699	0.031199	-6.239700	-94.419859	-27.022619
265	29.294500	0.038801	-7.760239	-102.180100	-34.782860
266	29.307501	0.013000	-2.600098	-104.780200	-37.382960
267	29.297001	-0.010500	2.099991	-102.680210	-35.282970
268	29.292299	-0.004702	0.940323	-101.739880	-34.342640
269	29.305700	0.013401	-2.680206	-104.420090	-37.022850
270	29.352400	0.046700	-9.339905	-113.759990	-46.362750
271	29.354401	0.002001	-0.400162	-114.160160	-46.762920
272	29.356400	0.001999	-0.399780	-114.559940	-47.162700
273	29.367399	0.011000	-2.199936	-116.759870	-49.362630
274	29.369600	0.002201	-0.440216	-117.200090	-49.802850

Section II. Data collected, averaged and calculated for all six acoustic rays. Columns per the following description:

Column A: JULIAN DATE - 189 and 274 correspond to July 7 and 1 October 1990, respectively.

Column B: ACOUSTIC TRAVEL TIME measurement in seconds - average of all six rays (Note: a constant value has been subtracted).

Column C: 24-HOUR ACOUSTIC TRAVEL ΔT in seconds (current value minus value from previous day).

Column D: 24-HOUR ΔR in kilometers, calculated from the value in column C.

Column E: CUMULATIVE ΔR in kilometers (summation of current and all previous values in column D).

Column F: CUMULATIVE ΔR in kilometers (value in column E minus the average of all values in column E).

A	B	C	D	E	F
189	29.686899	0.036900	-7.379913	-7.379913	55.876649
190	29.725800	0.038900	-7.780075	-15.159988	48.096574
191	29.825300	0.099501	-19.900131	-35.060119	28.196443
192	29.889799	0.064499	-12.899780	-47.959899	15.296663
193	29.944799	0.055000	-11.000061	-58.959960	4.296602
194	29.996799	0.052000	-10.400009	-69.359969	-6.103407
195	30.066000	0.069201	-13.840103	-83.200072	-19.943510
196	30.128901	0.062901	-12.580109	-95.780181	-32.523619
197	30.132601	0.003700	-0.740051	-96.520232	-33.263670
198	30.121500	-0.011101	2.220154	-94.300078	-31.043516
199	30.087299	-0.034201	6.840134	-87.459944	-24.203382
200	30.053499	-0.033800	6.760025	-80.699919	-17.443357
201	30.049500	-0.004000	0.799942	-79.899977	-16.643415
202	30.014799	-0.034700	6.940079	-72.959898	-9.703336
203	29.990000	-0.024799	4.959869	-68.000029	-4.743467
204	29.959600	-0.030399	6.079865	-61.920164	1.336398
205	29.936199	-0.023401	4.680252	-57.239912	6.016650
206	29.945000	0.008801	-1.760101	-59.000013	4.256549
207	29.979401	0.034401	-6.880188	-65.880201	-2.623639
208	30.040001	0.060600	-12.120056	-78.000257	-14.743695
209	30.111601	0.071600	-14.319992	-92.320249	-29.063687
210	30.098101	-0.013500	2.700043	-89.620206	-26.363644

Section II (continued)

A	B	C	D	E	F
211	30.034100	-0.064001	12.800217	-76.819989	-13.563427
212	29.966299	-0.067801	13.560104	-63.259885	-0.003323
213	29.921200	-0.045099	9.019852	-54.240033	9.016529
214	29.868799	-0.052401	10.480118	-43.759915	19.496647
215	29.789801	-0.078999	15.799713	-27.960202	35.296360
216	29.720301	-0.069500	13.899994	-14.060208	49.196354
217	29.631800	-0.088501	17.700195	3.639987	66.896549
218	29.553301	-0.078499	15.699768	19.339755	82.596317
219	29.496000	-0.057301	11.460114	30.799869	94.056431
220	29.480400	-0.015600	3.120041	33.919910	97.176472
221	29.495199	0.014799	-2.959824	30.960086	94.216648
222	29.524099	0.028900	-5.780029	25.180057	88.436619
223	29.553400	0.029301	-5.860138	19.319919	82.576481
224	29.581200	0.027800	-5.559921	13.759998	77.016560
225	29.607800	0.026600	-5.319977	8.440021	71.696583
226	29.618700	0.010900	-2.180099	6.259922	69.516484
227	29.648500	0.029800	-5.960083	0.299839	63.556401
228	29.687401	0.038900	-7.780075	-7.480236	55.776326
229	29.729700	0.042299	-8.459854	-15.940090	47.316472
230	29.819799	0.090099	-18.019867	-33.959957	29.296605
231	29.927299	0.107500	-21.500015	-55.459972	7.796590
232	30.056700	0.129400	-25.880051	-81.340023	-18.083461
233	30.123800	0.067101	-13.420105	-94.760128	-31.503566
234	30.169701	0.045900	-9.180069	-103.940200	-40.683638
235	30.187599	0.017899	-3.579712	-107.519910	-44.263348
236	30.193100	0.005501	-1.100159	-108.620070	-45.363508
237	30.181499	-0.011600	2.320099	-106.299970	-43.043408
238	30.147800	-0.033699	6.739807	-99.560162	-36.303600
239	30.104500	-0.043301	8.660126	-90.900036	-27.643474
240	30.057501	-0.046999	9.399796	-81.500240	-18.243678
241	30.045799	-0.011702	2.340317	-79.159923	-15.903361
242	30.077200	0.031401	-6.280136	-85.440059	-22.183497
243	30.111000	0.033800	-6.760025	-92.200084	-28.943522
244	30.161501	0.050501	-10.100174	-102.300260	-39.043698
245	30.198299	0.036798	-7.359695	-109.659950	-46.403388
246	30.242800	0.044500	-8.900070	-118.560020	-55.303458
247	30.247200	0.004400	-0.880051	-119.440070	-56.183508
248	30.212099	-0.035101	7.020187	-112.419890	-49.163328
249	30.185101	-0.026999	5.399704	-107.020180	-43.763618
250	30.138300	-0.046801	9.360123	-97.660060	-34.403498
251	30.101299	-0.037001	7.400131	-90.259929	-27.003367
252	30.063200	-0.038099	7.619858	-82.640071	-19.383509
253	30.028400	-0.034800	6.959915	-75.680156	-12.423594

Section II (continued)

A	B	C	D	E	F
254	29.996500	-0.031900	6.380081	-69.300075	-6.043513
255	29.987200	-0.009300	1.860046	-67.440029	-4.183467
256	29.998400	0.011200	-2.239990	-69.680019	-6.423457
257	29.988199	-0.010201	2.040100	-67.639919	-4.383357
258	29.983500	-0.004700	0.939941	-66.699978	-3.443416
259	29.973000	-0.010500	2.099991	-64.599987	-1.343425
260	29.967699	-0.005301	1.060104	-63.539883	-0.283321
261	29.967699	0.000000	0.000000	-63.539883	-0.283321
262	29.972500	0.004801	-0.960159	-64.500042	-1.243480
263	29.981501	0.009001	-1.800156	-66.300198	-3.043636
264	30.007700	0.026199	-5.239868	-71.540066	-8.283504
265	30.045099	0.037399	-7.479858	-79.019924	-15.763362
266	30.062000	0.016901	-3.380203	-82.400127	-19.143565
267	30.028500	-0.033501	6.700134	-75.699993	-12.443431
268	30.028000	-0.000500	0.099945	-75.600048	-12.343486
269	30.046400	0.018400	-3.680038	-79.280086	-16.023524
270	30.086100	0.039700	-7.939911	-87.219997	-23.963435
271	30.100401	0.014301	-2.860260	-90.080257	-26.823695
272	30.132601	0.032200	-6.439972	-96.520229	-33.263667
273	30.135799	0.003199	-0.639725	-97.159954	-33.903392
274	30.138599	0.002800	-0.559998	-97.719952	-34.463390

Section III: Data collected from the NAVOCEANO OOC Gulf Stream analysis based on satellite IR imagery, for the ray path intersection with the north wall of the Gulf Stream. Columns per the following description:

Column A: JULIAN DATE - 189 and 274 correspond to 7 July and 1 October 1990, respectively.

Column B: 24-HOUR NAVOCEANO OOC DELTA-R in kilometers for the ray path intersection with the north wall as taken from the Composite Gulf Stream Analysis (GSCOMP).

Column C: CUMULATIVE NAVOCEANO OOC DELTA-R in kilometers (summation of current and all previous values in column B).

Column D: CUMULATIVE NAVOCEANO OOC DELTA-R in kilometers (column C value minus the average of all column C values).

A	B	C	D
189	55.560	55.560	48.195
190	55.560	111.120	103.755
191	-27.780	83.340	75.975
192	-27.780	55.560	48.195
193	-22.224	33.336	25.971
194	-22.224	11.112	3.747
195	0.000	11.112	3.747
196	5.556	16.668	9.303
197	5.556	22.224	14.859
198	0.000	22.224	14.859
199	0.000	22.224	14.859
200	-11.112	11.112	3.747
201	-11.112	0.000	-7.365
202	-16.668	-16.668	-24.033
203	0.000	-16.668	-24.033
204	16.668	0.000	-7.365
205	0.000	0.000	-7.365
206	22.224	22.224	14.859
207	0.000	22.224	14.859
208	22.224	44.448	37.083
209	0.000	44.448	37.083
210	0.000	44.448	37.083
211	-11.112	33.336	25.971
212	0.000	33.336	25.971
213	-5.556	27.780	20.415
214	0.000	27.780	20.415

Section III (continued)

A	B	C	D
215	-5.556	22.224	14.859
216	-5.556	16.668	9.303
217	5.556	22.224	14.859
218	11.112	33.336	25.971
219	0.000	33.336	25.971
220	11.112	44.448	37.083
221	0.000	44.448	37.083
222	-22.224	22.224	14.859
223	0.000	22.224	14.859
224	33.336	55.560	48.195
225	-22.224	33.336	25.971
226	5.556	38.892	31.527
227	-5.556	33.336	25.971
228	0.000	33.336	25.971
229	-88.896	-55.560	-62.925
230	0.000	-55.560	-62.925
231	11.112	-44.448	-51.813
232	-11.112	-55.560	-62.925
233	0.000	-55.560	-62.925
234	-44.448	-100.010	-107.380
235	-11.112	-111.120	-118.480
236	-11.112	-122.230	-129.590
237	33.336	-88.896	-96.261
238	55.560	-33.336	-40.701
239	0.000	-33.336	-40.701
240	-11.112	-44.448	-51.813
241	-11.112	-55.560	-62.925
242	0.000	-55.560	-62.925
243	11.112	-44.448	-51.813
244	-11.112	-55.560	-62.925
245	0.000	-55.560	-62.925
246	-11.112	-66.672	-74.037
247	0.000	-66.672	-74.037
248	55.560	-11.112	-18.477
249	55.560	44.448	37.083
250	-44.448	0.000	-7.365
251	-44.448	-44.448	-51.813
252	-11.112	-55.560	-62.925
253	55.560	0.000	-7.365
254	11.112	11.112	3.747
255	0.000	11.112	3.747
256	11.112	22.224	14.859
257	-11.112	11.112	3.747

Section III (continued)

A	B	C	D
258	-11.112	0.000	-7.365
259	-5.556	-5.556	-12.921
260	16.668	11.112	3.747
261	22.224	33.336	25.971
262	16.668	50.004	42.639
263	16.668	66.672	59.307
264	0.000	66.672	59.307
265	33.336	100.008	92.643
266	0.000	100.008	92.643
267	-55.560	44.448	37.083
268	0.000	44.448	37.083
269	-11.112	33.336	25.971
270	0.000	33.336	25.971
271	-11.112	22.224	14.859
272	0.000	22.224	14.859
273	0.000	22.224	14.859
274	0.000	22.224	14.859

DISTRIBUTION LIST

1. Office of Naval Research
   Code 1242 (10 copies)
   800 North Quincy Street
   Arlington, VA 22217-5000

2. Director, Atmospheric Sciences
   Directorate
   NOARL West (Code 400)
   Monterey, CA 93943-5000

3. Commanding Officer
   Fleet Numerical Oceanography Office
   Monterey, CA 93943-5000

4. Commanding Officer
   Naval Oceanographic Office
   Stennis Space Center, MS 39529

5. Technical Director
   CNOC (Code OOT)
   Stennis Space Center, MS 39529

6. Commanding Officer
   NOARL (Code 100)
   Stennis Space Center, MS 39529

7. Technical Director
   NOARL (Code 110)
   Stennis Space Center, MS 39529

8. Director, Ocean Sciences
   Directorate
   NOARL (Code 300)
   Stennis Space Center, MS 39529

9. Head, Ocean Sensing and
   Prediction Division
   NOARL (Code 320)
   Stennis Space Center, MS 39529

10. Library (3 copies)
    NOARL (Code 125)
    Stennis Space Center, MS 39529

11. Dr. J. Dana Thompson
    NOARL, Code 320
    Building 1103, Room 248
    Stennis Space Center, MS 39529

12. Dr. William J. Schmitz, Jr.
    Department of Oceanography
    Woods Hole Oceanographic Inst.
    Woods Hole, MA 02543

13. Dr. William Holland
    National Center for Atmospheric
    Research
    P. O. Box 3000
    Boulder, CO 80307

14. UCAR Library
    P. O. Box 3000
    Boulder, CO 80307

15. Dr. Bruce Howe
    Applied Physics Laboratory
    University of Washington
    1013 NE 40th Street
    Seattle, WA 98107

16. Dr. John Spiesberger
    Woods Hole Oceanographic Inst.
    Woods Hole, MA 02543

17. Mr. Robert Winokur
    Chief of Naval Operations
    Code 096T
    U.S. Naval Observatory
    34th & Massachusetts Ave., NW
    Washington, DC 20392-1800

18. Dr. Bruce Cornuelle
    Scripps Institution of Oceanography
    LaJolla, CA 92093

19. Mr. K.W. Lackie
    Office of Naval Research, Code 124D
    800 N. Quincy Street
    Arlington, VA 22217-5000

20. Naval Oceanographic Office
    CDR C. Hall, Code OC
    Mr. Robert Moshier, Code OC
    Mr. Zaaron Allan, Code OC
    Stennis Space Center, MS 39529

21. NOARL
    Code 100, 110, 125L, 125P, 300,
    320, 321, 322, 323, 331
    Stennis Space Center, MS 39529

REPORT DOCUMENTATION PAGE

Form Approved OMB No. 0704-0188

1. Agency Use Only *(Leave blank).*	2. Report Date.	3. Report Type and Dates Covered.
	October 1991	Technical Memo

4. Title and Subtitle.
The Utility of Acoustic Travel Times in Locating the North Wall of the Gulf Stream

5. Funding Numbers.
Program Element No. 0603785N
Project No. 00120
Task No. 809
Accession No. Internal

6. Author(s).
Michael S. Foster, CDR, USN

7. Performing Organization Name(s) and Address(es).
Institute for Naval Oceanography
Building 1103, Room 233
Stennis Space Center, MS 39529-5005

8. Performing Organization Report Number.
TM-5

9. Sponsoring/Monitoring Agency Name(s) and Address(es).
Naval Oceanographic and Atmospheric Research Laboratory
Stennis Space Center, MS 39529

10. Sponsoring/Monitoring Agency Report Number.

11. Supplementary Notes.

12a. Distribution/Availability Statement.
Approved for public release; distribution is unlimited.

12b. Distribution Code.

13. Abstract *(Maximum 200 words).*

Eighty-seven days of travel time data for ocean acoustic transmissions across the north wall of the Gulf Stream were examined. The data was collected from 7 July to 1 October 1990 during the 1990 Applied Tomography Experiment (ATE90), sponsored by the Chief of Naval Research. The acoustic ray paths were, generally, perpendicular to the north wall. The analysis indicates that acoustic ray travel times can be useful in locating ocean frontal features and in reliably augmenting subjective techniques based on infrared (IR) satellite imagery and bathythermograph (BT) data. This document presents the procedures employed during the study and discusses the results.

14. Subject Terms.
(U) Acoustic Tomography (U) Mesoscale Oceanography
(U) Ocean Forecasting (U) INO

15. Number of Pages. 22

16. Price Code.

17. Security Classification of Report.	18. Security Classification of This Page.	19. Security Classification of Abstract.	20. Limitation of Abstract.
Unclassified	Unclassified	Unclassified	SAR